Highlights

Experimental investigation into the role of nonlinear suspension behaviour in limiting feedforward road noise cancellation

Matthew de Brett, Tore Butlin, Luis Andrade, Ole M. Nielsen

- Car tests highlight role of nonlinearity in limiting coherence of reference signals
- Dynamics of hydraulic dampers shown to be strongly nonlinear at low audio frequencies
- Damper nonlinearity appears to limit the performance of a feedforward controller

Experimental investigation into the role of nonlinear suspension behaviour in limiting feedforward road noise cancellation

Matthew de Brett[a,*], Tore Butlin[a], Luis Andrade[a], Ole M. Nielsen[a,b]

[a]*Department of Engineering, University of Cambridge, Cambridge, UK*
[b]*Bose Corporation, Framingham, MA, USA*

Abstract

Feedforward control of road noise in cars is limited by the difficulty of finding reference signals that have adequate coherence with the sound at the passenger head positions. The dynamics of car suspensions are known to be nonlinear and could therefore restrict the coherence between reference and error sensors and limit the performance of linear feedforward road noise control systems. This paper presents two sets of experiments that investigate nonlinear vibration transmission through a car suspension and its implications for road noise control. The first experiment was conducted on an electric car; an analysis of the maximum theoretical cancellation that can be achieved with different sets of reference signals is presented and the influence of 'smooth' and 'rough' road surfaces is investigated. In the second set of experiments, components from the car's suspension systems are tested in a laboratory. The experiments show that the car's hydraulic dampers are strongly nonlinear at low audio frequencies, and suggest that they limit the cancellation that can be achieved with a linear controller.

Keywords: Road noise, active noise control, nonlinear vibration, random vibration, feedforward control

1. Introduction

Interior road noise influences customer perception of cars and is an increasingly important design consideration for manufacturers. Random broadband vibration is generated at the tyre-road interface and is transmitted into the cabin via structure-borne and airborne mechanisms. The structure-borne component consists of vibration that propagates through the suspension systems into the car's body which then radiates sound into the cabin, and it is the dominant source of interior noise below 500 Hz [1][2]. The low frequency nature of structure-borne road noise makes it difficult to control with passive techniques that are commonly used in cars, such as viscoelastic damping treatments applied to body panels or porous materials in the cabin. These are less effective at low frequencies where the wavelength of sound and vibration becomes comparable to the thickness of the material [3]. In contrast, active techniques are most effective at low frequencies and therefore appear to be well suited to reducing structure-borne road noise in cars.

Active noise control (ANC) has long been investigated as a means of mitigating both engine and road noise in cars [4][5][6]. Fundamentally, ANC systems use controllable secondary sources to try to cancel a primary disturbance. Although vibration control with mechanical actuators is a viable strategy for ANC in cars [7][8], the system considered in this research uses loudspeakers to cancel the sound at the passenger head positions. Global control with loudspeakers, in which the sound is reduced throughout the entire cabin, is limited to frequencies below 300 Hz [9]. Cancellation at higher frequencies can be achieved using a local control strategy, in which zones of quiet are generated around the passenger head positions [6]. When paired with head-tracking technology, local control could extend the controllable frequency range towards 1 kHz [10][11].

Active engine control systems that aim to cancel the fundamental tone and harmonics of the engine are well established and a number have been deployed commercially [12][13]. The engine's rotational speed can be obtained from

*Corresponding author: Matthew de Brett, Department of Mechanical Engineering, City and Guilds Building, Imperial College London, Exhibition Road, London, SW7 9AG, UK. Email: m.de-brett@imperial.ac.uk

the vehicle's Controller Area Network bus and input to a feedforward controller, that is adaptive to track changes in the acoustic field caused by engine speed and load variations during driving [5][14]. Active control of road noise is more complicated because of the random and broadband nature of the input disturbance. Both feedback and feedforward strategies have been investigated in road noise control (RNC) systems. In this study a feedforward strategy is considered for two main reasons: it enables selective attenuation and lacks the stability trade-off inherent in feedback systems, which could limit the control bandwidth of a feedback controller [6].

In linear feedforward RNC systems, accelerometers are placed on the suspension or chassis to provide reference signals for the controller, which drives a number of loudspeakers. Error microphones are placed in the cabin to measure the sound at the passenger head positions and adapt the controller. An essential stage in the design of feedforward RNC systems is the selection of reference sensors, which are chosen according to two main criteria [9]: reference sensors must be placed far enough from the error microphones (in the cabin) to allow an adequate time advance and ensure that the controller is causal; and the reference sensors should have high multiple coherence with the error microphones. Assuming that there is an adequate time advance, the theoretical maximum noise cancellation that can be achieved with a feedforward control system is governed by the multiple coherence between the reference signals and the error microphones in the cabin [15]. Finding reference sensor locations that maximise the multiple coherence is therefore a key stage in the design of a feedforward RNC system.

A variety of different methods have been used to select reference sensor locations, ranging from trial-and-error approaches [15][16][17] to the application of techniques such as principal component analyses or transfer path analyses [9][18][19][20]. Although reductions of up to 10 dB have been achieved over narrow frequency ranges [18][19], broadband cancellation tends to produce smaller reductions: Cheer and Elliott reported an average cancellation of 3 dB between 80-180 Hz [21] while Duan et al. reported a total reduction of 4 dBA between 50-500 Hz [17]. The difficulty of finding an optimal set of reference sensor locations motivates the question of what factors limit the coherence between reference sensors placed on the suspension and error microphones in the cabin. This research investigates the influence of nonlinearity in the transmission path of structure-borne road noise in limiting the performance of feedforward RNC systems. Nonlinear components in the road noise transmission path could cause vibration in the cabin that is uncorrelated with the reference signals and can not be cancelled using a linear controller.

Although the influence of nonlinear or time-changing system properties has been noted previously [4][15], a comprehensive analysis of their implications for feedforward control of road noise is lacking in the literature. This is in spite of the fact that the nonlinear dynamics of car suspensions have been researched extensively; the hydraulic dampers and rubber bushings found in the vast majority of car suspensions are known to behave nonlinearly [22][23][24][25]. Bushings are used at the connections between the suspension system and car body to prevent the wear of mechanical joints and reduce the transmission of vibrations from the road. Rubber is used because of its elastic and damping properties, with fillers such as carbon black added to increase fatigue life and abrasion resistance. The presence of fillers causes an amplitude dependence in the bushings known as the Payne effect [26][27], while a stiffness nonlinearity arises from the bushing geometry. Hydraulic dampers consist fundamentally of a piston moving through a cylinder filled with oil. The relative motion of the wheel and chassis forces the damper piston to move through the oil, and energy is dissipated through viscous fluid friction [28]. Hydraulic dampers display a range of complex mechanical and fluid effects. The rate of oil flow through an assembly of valves and restrictions in the piston head strongly influences the damping force; however, the behaviour of the valves at low velocities and the onset of additional blow-off valves at high pressures leads to a strongly nonlinear damping force [22][23]. Mechanical friction at the sliding interfaces between the piston rod and cylinder is also thought to be significant [23].

While the nonlinear behaviour of the hydraulic dampers and rubber bushings have been covered extensively in the literature, their relevance to feedforward RNC has not been properly addressed. This study presents experiments that aim to quantify the significance of damper and bushing nonlinear characteristics for feedforward RNC. In Section 2, the details of experiments conducted on an electric car are presented. Section 3 contains results from these that strongly suggest that nonlinearity in the road noise transmission path affects control performance. Finally, a set of laboratory experiments are presented in Section 4 that accurately quantify the extent of the dampers' and top mount bushing's nonlinear characteristics at low audio frequencies.

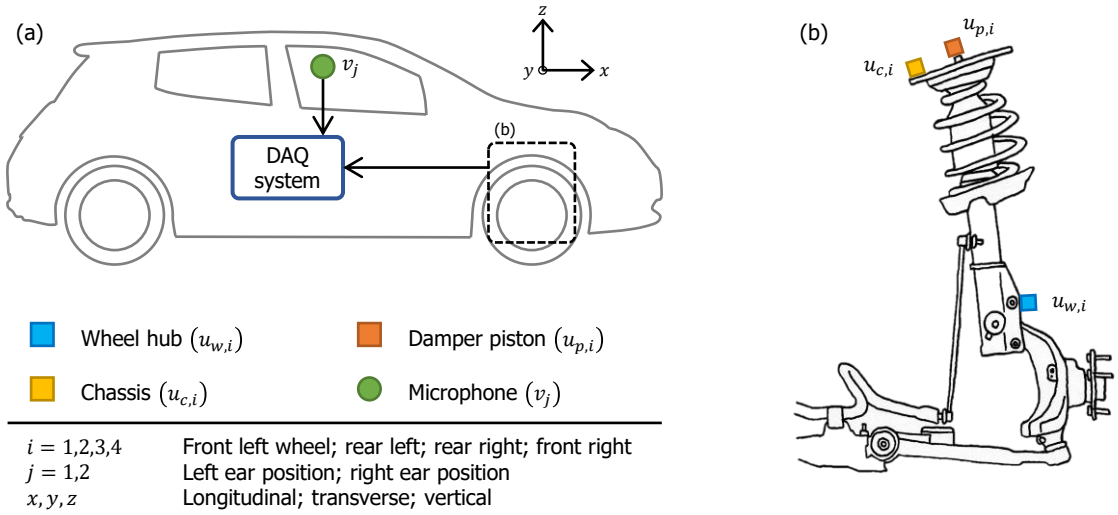

Figure 1: Diagrams of the DAQ system and sensor locations within (a) the car and (b) the front suspension. The table explains the sensor coordinate system.

2. Car test setup

A Nissan Leaf was chosen for the measurements because it has an electric motor, which means power train noise in the cabin is negligible when compared to wind or road noise. Since wind noise is most significant at high speeds, the contribution of road noise can be effectively isolated by testing the Nissan Leaf at speeds of approximately 30 mph. Vibration measurements were obtained at 12 locations on the car, together with measurements of sound at two positions in the cabin.

Figure 1 is a schematic diagram of the sensors and data acquisition (DAQ) system used in the car. Figure 1a shows the positions of these components within the car and explains the coordinate system. Two microphones, v_j, were positioned in the cabin and accelerometers were placed on each of the four suspension systems. The locations of the accelerometers on the front left suspension are shown in Fig. 1b. The front suspension in the Nissan Leaf is a MacPherson type, meaning that the wheel hub is attached to the chassis via three main structural connections. At the bottom of the diagram there is a wishbone that connects via two rubber bushings and at the top is the vertical strut, which consists of a damper and top mount bushing in parallel with a spring. Vibration is generated at the tyre-road interface and transmitted through the tyre to the wheel hub. Accelerometers were therefore placed on the wheel hubs to measure the incoming vibration. Vibration is then propagated into the chassis through each of the main connections, as well as the driveshaft, anti-roll bar and steering track rod. The high number of transmission paths in the front suspension means that measuring all the paths in every suspension is impractical. Instead of measuring each path, sensors were placed on the damper piston rod and chassis in the vertical struts. The displacements of the wheel hub, damper piston rod and chassis are denoted u_w, u_p and u_c respectively. It was decided to focus on the struts as they contain a damper and a rubber top mount bushing, which were identified in the literature as the most likely sources of nonlinearity in the suspensions [22][23][24][25]. The rear suspension system in the Nissan Leaf is different to the front and has a twist-beam configuration, which means that the left and right rear wheels are coupled. This configuration also contains a vertical strut on each side and so accelerometers were again placed on the damper piston rods and chassis.

The entire DAQ system must be powered from the single 12 V power outlet available in the car. To overcome this constraint, Integrated Electronics Piezoelectric sensors were used. PCB 356A16 triaxial accelerometers were placed at each of the three locations on each suspension, meaning that there are nine accelerometer channels on each corner of the car, and 36 in total. Figure 2 shows images of three of the accelerometers as fixed to the suspensions. The wheel hub accelerometers were glued to custom made mounting blocks that bolted to the hub (Fig. 2a,b), while the damper piston rod accelerometers were fixed via magnets to custom components that screwed on to the ends of

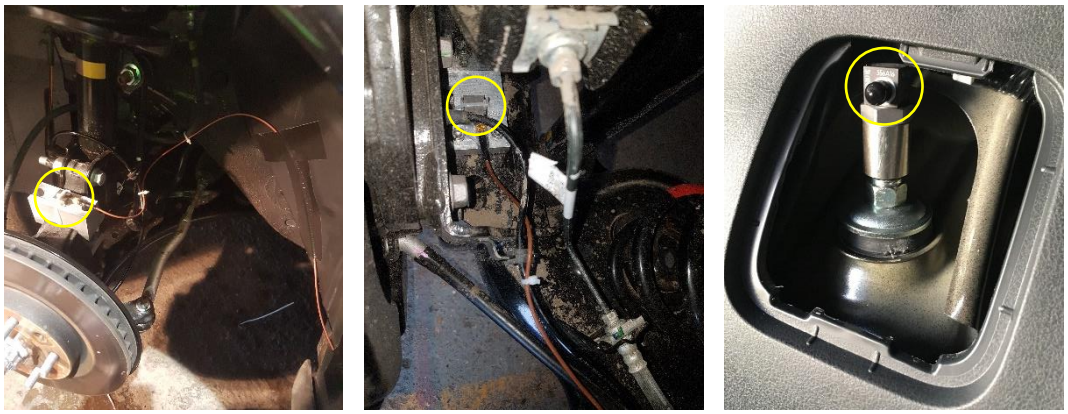

(a) (b) (c)

Figure 2: Photos of the accelerometers positioned on (a) the front left wheel hub $u_{w,1}$, (b) the rear right wheel hub $u_{w,3}$ and (c) the rear left damper piston rod $u_{p,2}$.

the piston rods (Fig. 2c). The chassis accelerometers were mounted directly onto the chassis using magnets. All of the accelerometers were positioned such that their axes aligned approximately with the coordinate system shown in Fig. 1a, so no additional coordinate transformations were required when processing the signals. Two PCB 130F21 microphones were mounted on a headband, worn by the front passenger, to measure the sound at the front passenger's ear positions. Mounting the microphones on a headband may mean that the sound measurements are affected by head movements, however, this setup is felt to be an accurate representation of the real RNC problem. In total, this sensor configuration provides 38 channels of data.

The DAQ system was designed to be capable of sampling 32 measurement channels at 20 kHz while being powered from the car's 12 V power outlet. Two 16 channel custom-made signal conditioning units (SCU) were used to provide suitable bias voltages to the sensors. The SCU also applies a gain and low-pass filter to each of the sensor signals. The gains were selected to scale the incoming signals to have amplitudes on the order of 1 V, as the data logger had a maximum input voltage of ± 10 V. Low-pass filters were set with 8^{th} order roll-offs at 7.4 kHz to prevent aliasing. The SCUs only allow for 32 channels, meaning six had to be omitted for any single set of measurements. To overcome this limitation, several recordings were made with different combinations of omitted channels, to ensure that all locations were measured. All the results presented in this paper are derived from a single data set (making them directly comparable) apart from those containing measurements on the rear chassis connections $u_{c,2-3}$. To ensure that good comparisons could be made between the two data sets, a large volume of data was collected and averaged across for each measurement configuration.

A National Instruments (NI) Compact Reconfigurable Input/Output-9037 (cRIO) system was used to log data from the sensors. The cRIO contains a real-time processor that interfaces with customisable input/output modules via a Field-Programmable Gate Array (FPGA). The cRIO was chosen as it provides the capacity to implement a controller: the FPGA is capable of processing data at high speeds and is therefore well suited to active noise control applications in which time delays are critical. However in this study, the cRIO was only required for collecting data from the car so two NI-9220 analogue voltage input modules, which incorporate 16 bit analogue-to-digital converters, were connected to it. The FPGA was programmed to pass data directly to the real-time processor, which in turn streamed data to a laptop. A graphical user interface on the laptop displayed the most recent 30 s of data on a graph and enabled data to be saved.

3. Car test results

Data was collected as the car was driven on local roads at speeds of approximately 30 mph. The roads were chosen on the basis that they had speed limits of 30 mph, were in generally good condition and had relatively little traffic (making measurements easier); however, since the measurements are intended to be averaged, the exact details of the

roads and surfaces are not important. The experiments conducted on the car provided two important results that are presented in this section. First, multiple coherence plots are shown when calculated with different combinations of input signals. Then the data is split into 'smooth' and 'rough' road categories and coherences are calculated for each category.

3.1. Multiple coherence and theoretical control limit

The multiple coherence between a set of inputs, U, and an output, V_j, is calculated by first assembling an augmented cross-spectrum matrix $\mathbf{S}_{VUU}$, where the capitalised U and V denote Fourier transforms of u and v. If I accelerometer signals are taken as inputs, and two microphone signals as outputs, then for each output V_j,

$$\mathbf{S}_{V_jUU} = \begin{bmatrix} S_{V_jV_j} & \mathbf{S}_{V_jU} \\ \mathbf{S}_{V_jU}^{\mathrm{H}} & \mathbf{S}_{UU} \end{bmatrix} \tag{1}$$

is the augmented cross-spectrum matrix of the inputs and outputs, where $\mathbf{S}_{UU} = \mathrm{E}[UU^{\mathrm{H}}]$ is the I-by-I cross-spectrum matrix of the inputs and E denotes the expectation; $\mathbf{S}_{VV} = \mathrm{E}[VV^{\mathrm{H}}]$ is the 2-by-2 cross-spectrum matrix of the outputs; $\mathbf{S}_{VU} = \mathrm{E}[VU^{\mathrm{H}}]$ is the 2-by-I cross-spectrum matrix of the inputs and outputs; and $\cdot^{\mathrm{H}}$ denotes the Hermitian transpose. Note that $S_{V_jV_j}$ refers to the PSD of the output V_j and $\mathbf{S}_{V_jU}$ denotes the cross-spectrum matrix of the inputs U and output V_j. The multiple coherence from the inputs to each output is [29]

$$\gamma^2_{V_jU} = 1 - \frac{\left|\mathbf{S}_{V_jUU}\right|}{S_{V_jV_j}\left|\mathbf{S}_{UU}\right|} = \frac{1}{S_{V_jV_j}}\mathbf{S}_{V_jU}\mathbf{S}_{UU}^{-1}\mathbf{S}_{V_jU}^{\mathrm{H}}, \tag{2}$$

where $|\mathbf{S}|$ denotes the determinant of the matrix $\mathbf{S}$, and $\gamma^2_{V_jU}$ represents the maximum fraction of the energy in output V_j that can theoretically be cancelled with a linear controller using the inputs U as reference signals. This gives the maximum possible sound power reduction in decibels [4], which will be referred to as the coherence limit Γ^2, as

$$\Gamma^2_{V_jU} = 10\log(1 - \gamma^2_{V_jU}). \tag{3}$$

The Power Spectral Densities (PSDs) and multiple coherences were calculated by averaging over 25 data sets, sampled at 20 kHz and lasting 30 s. The data was split into frames of length 1.6 s (2^{15} samples) and Hann windows were applied with an overlap of half the frame length. The frame lengths were chosen to be long enough to provide good frequency resolution down to the lower limits of the accelerometer operating ranges, but short enough to allow sufficient averaging across frames. Frames were averaged across data sets to provide representative measurements for a variety of roads. All spectra were calculated from 25 data sets, which each provided 35 frames of data, meaning 875 frames contribute to each PSD.

Figure 3a shows the multiple coherence $\gamma^2_{V_1U}$ to the left microphone position, V_1, when calculated with different sets of inputs: the solid (blue) line is the coherence with all the wheel hub accelerometer channels, $U_{w,1-4,x-z}$, taken as inputs; the dashed (red) line has the damper piston rod accelerometers, $U_{p,1-4,x-z}$, as inputs; and the dot-dashed (yellow) line has both of these sets of accelerometers as inputs. The coherence calculated with just $U_{p,1-4,x-z}$ as inputs (dashed, red) is in general slightly higher than the coherence calculated with just $U_{w,1-4,x-z}$ as inputs (solid, blue) in the range of 30-230 Hz. The difference between these lines is typically 0.05-0.1 across this frequency range, although the coherence calculated with $U_{p,1-4,x-z}$ is significantly higher around 70 Hz. The overall trend could perhaps be explained by the damper piston rod being more strongly coupled to the chassis than the wheel is, so that the accelerometer is measuring noise from other sources. It is also possible that nonlinearity in the dampers degrades the coherence when $U_{w,1-4,x-z}$ are taken as inputs, which is partially compensated by measuring inputs at the tops of the dampers.

When both $U_{w,1-4,x-z}$ and $U_{p,1-4,x-z}$ are taken as inputs (dot-dashed, yellow), a further, significant improvement is seen in the multiple coherence. This suggests that some road noise is transmitted through other paths (e.g., lower bushings, springs and anti-roll bar) that may not be detected by accelerometers placed at $U_{p,1-4}$. This illustrates the benefit of obtaining reference signals at the wheel hubs, as it enables the measurement of all of the vibrations induced at the tyres.

Figure 3b shows the coherence limits corresponding to the coherences plotted in Fig. 3a. These are equivalent to the maximum cancellation at V_1 that is theoretically possible with a linear control system using each set of reference signals. In practice, once a controller is fitted with a constraint on causality the actual cancellation would be less;

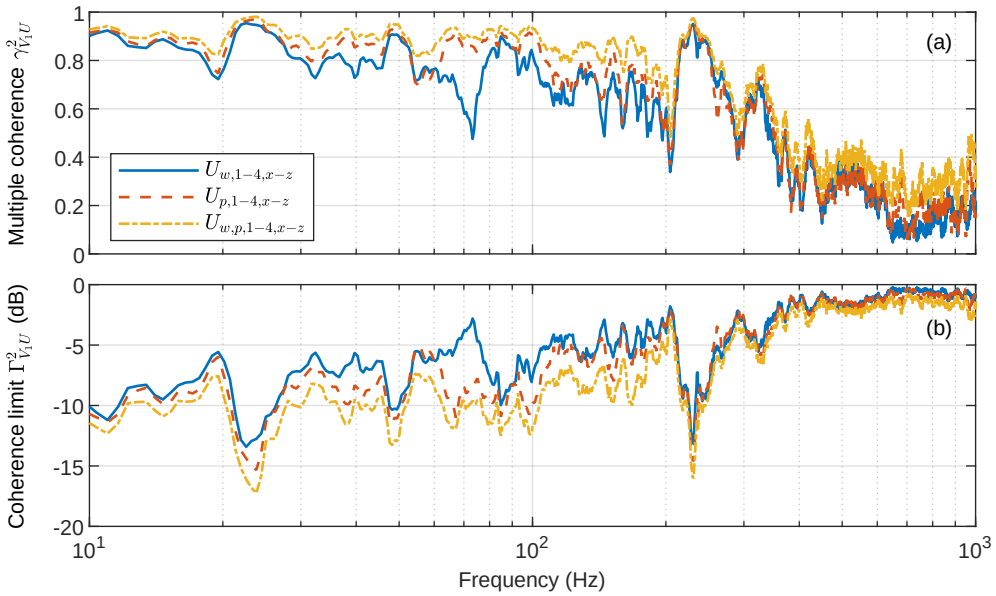

Figure 3: (a) Multiple coherence and (b) coherence limit with different combinations of $U_{w,1-4,x-z}$ and $U_{p,1-4,x-z}$ taken as inputs and V_1 as the output.

nevertheless it is a useful metric for the maximum possible performance. The most cancellation is given by the set containing all the accelerometers $U_{w,1-4,x-z}$ and $U_{p,1-4,x-z}$ (dot-dashed, yellow). With these accelerometers, the cancellation that can theoretically be achieved is between 5-13 dB in the 50-200 Hz frequency range. However, this level of cancellation requires 24 accelerometer signals, which is unrealistic for a commercial RNC system, which may be limited to 8-10 reference signals. The two sets containing 12 input signals, $U_{w,1-4,x-z}$ (solid, blue) and $U_{p,1-4,x-z}$ (dashed, red) are therefore more realistic representations of a real RNC system. Of these, the set measured on the damper piston rods, $U_{p,1-4,x-z}$, gives the most cancellation. However, it is also clear that placing the reference sensors here can only provide somewhat limited noise reduction. The coherence limits shown in Fig. 3b are in line with other results reported in the literature [17][21]; although reductions of up to 10 dB might be possible at some frequencies, the actual cancellation above 100 Hz would most likely be restricted to below 5 dB (apart from the peak at 230 Hz). Cancellation approaching 10 dB in this range is desirable in order to take full advantage of the advances in local control described in Section 1 [10][11]. However, achieving this level of cancellation using a limited number of sensors (e.g., 8-10) and a linear control system appears to be impossible.

Figure 3 highlights the difficulty of finding an optimal set of reference sensors. One possible explanation for the trends seen in Fig. 3 is nonlinearity in the transmission paths between $U_{w,1-4}$ and V_1; nonlinear components in the suspension could cause a component of vibration in the cabin that is uncorrelated with the reference sensors placed at the wheels, which can not be cancelled using a linear control system. However, the presence of other noise sources in the microphone measurement, V_1, mean the trends in coherence can not be definitively attributed to nonlinearity. Additionally, although the microphones were kept as still as possible, small head movements could have also contributed to the degradation in coherence. Further insight into the role of nonlinear suspension behaviour in limiting the coherences plotted in Fig. 3a can be gained by calculating the coherence between the accelerometers placed on the wheel hubs and those on the damper piston rods and chassis. If the suspension's dynamics are nonlinear, these coherences should also be less than 1.

Figure 4 shows the multiple coherence to the vertical (z) axes of the damper piston rod and chassis in the front left suspension. In both cases, the multiple coherence has been calculated with different sets of inputs: the vertical channel of the front left wheel hub accelerometer $U_{w,1,z}$ (solid, light blue); all three axes of the front left wheel hub accelerometer $U_{w,1,x-z}$ (dashed, mid blue); and every axis of all four wheel hub accelerometers $U_{w,1-4,x-z}$ (dot-dashed, dark blue). By plotting the progression of the multiple coherence as more inputs are added, it is possible to see where

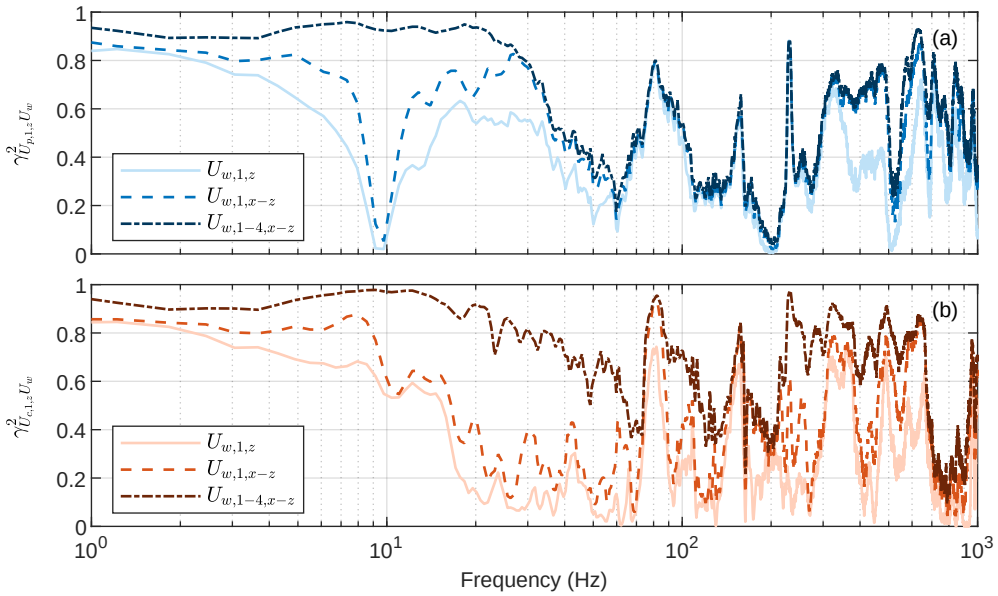

Figure 4: Multiple coherences from different sets of wheel hub accelerometers U_w to the vertical axes of (a) the front left damper piston rod $U_{p,1,z}$ and (b) the front left chassis $U_{c,1,z}$.

the energy in the outputs comes from. At all frequencies, the coherence improves from the lightest shade line to the darkest shade as more input channels are included in the calculation. The difference between two lines - for instance, between the light blue and mid blue lines in Fig. 4a - is indicative of how much energy is contained in the additional channels ($U_{w,1,xy}$ in this case) that is linearly correlated with the output and not contained in the lighter line's channels ($U_{w,1,z}$ in this case). Although this approach gives some insight into the sources that cause vibration at the chassis and damper piston rod, it does not precisely define each of the wheel channels' contributions.

The multiple coherence between the front left wheel signals and the piston rod is very low at 10 Hz (solid, mid blue), suggesting little energy is transmitted through the vertical strut at this frequency (Fig. 4a). When the other wheels are added as inputs (dot-dashed, dark blue), the coherence improves to above 0.9 at low frequencies; further analysis revealed that most of this energy is derived from the x axes of the rear wheels. Above 30 Hz, the coherence is low even when all of the channels are included (dot-dashed, dark blue). This is caused either by nonlinearity in the vertical strut or noise from other sources. The fact that the other wheels do not improve the coherence above 30 Hz, particularly when compared to the chassis coherence plot in Fig. 4b, suggests that the accelerometer placed on the damper piston rod is well isolated from the chassis and therefore does not detect much noise from other sources in this frequency range. This therefore strongly suggests that suspension nonlinearity is responsible for the low coherence in Fig. 4a, although this can not be stated with certainty. The peaks at 80 Hz and 230 Hz are caused by modes of the tyre, while the peak at 165 Hz appears to be related to the strut's lateral dynamics. Above 300 Hz, coherence is improved by including the x and y axes of the front left wheel as inputs (solid, mid blue). These axes appear to be more significant at higher frequencies.

Figure 4b shows the same set of plots with the vertical axis of the chassis accelerometer, $U_{c,1,z}$, as the output. Above 10 Hz, the coherence between the front left wheel and the chassis is generally very low (dashed, medium red). Coherence is significantly improved at most frequencies when the other three wheels are included as inputs (dot-dashed, dark red), which suggests that the accelerometer placed on the chassis is affected by noise from other sources. Even when all 12 signals from the wheel hubs are included, the multiple coherence is significantly less than 1 above 20 Hz. Although this could be due in part to nonlinearity in the suspension systems, noise from other sources is also likely to be somewhat responsible. Given that the chassis accelerometer detects vibration stemming from the other three wheels, it could also measure unwanted sources such as power train and wind noise.

Figure 5 shows the same sequence of plots for the rear left suspension. The multiple coherences to the damper

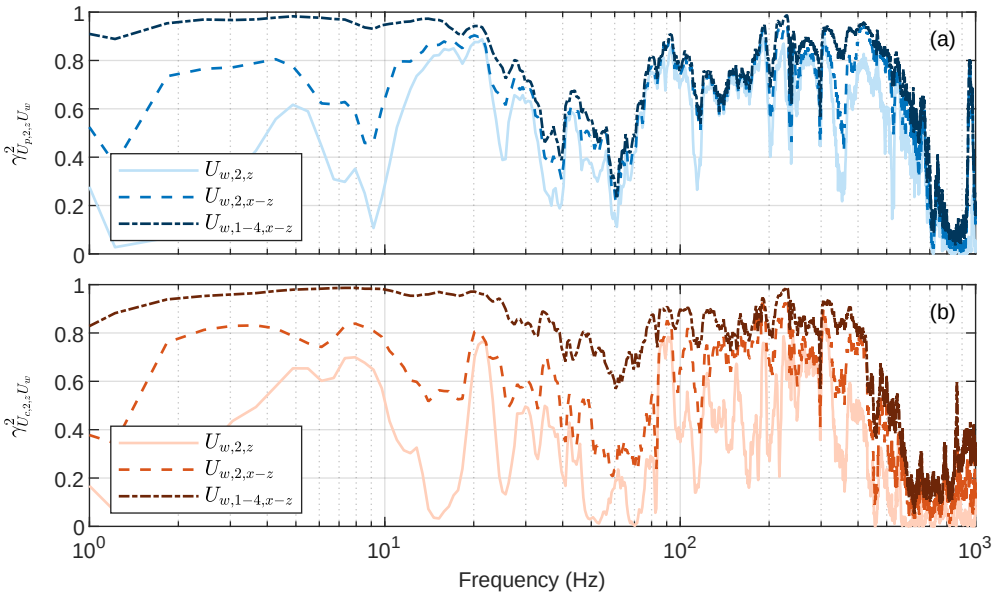

Figure 5: Multiple coherences from different sets of wheel hub accelerometers U_w to the vertical axes of (a) the rear left damper piston rod $U_{p,2,z}$ and (b) the rear left chassis $U_{c,2,z}$.

piston rod are in general higher than in the front left suspension (Fig. 5a). Like in the front, the coherence decreases between 20-80 Hz. However, above this frequency range the coherence is quite high, even if only the z axis of the rear left wheel is used as an input. Between 200-500 Hz, the coherence with all channels as inputs (dot-dashed, dark blue) is above 0.8 at nearly every frequency. Once again, the other wheels do not improve the coherence in the 20-200 Hz range where coherence is lowest. This suggests that the piston rod accelerometer in the rear left suspension is isolated from other noise sources and so nonlinear suspension behaviour is the cause of the low coherence. It also appears that the rear damper is less strongly nonlinear than the front for the excitations seen in the car. The multiple coherences to the chassis are also higher in the rear left suspension than the front left, in particular above 80 Hz (Fig. 5b). This might be because the rear damper is less nonlinear than the front, however, it could also be a result of the different suspension configuration used in the rear; the rear suspension has a twist-beam axle, which means that the two rear wheels are coupled. Another factor that may cause the coherence to be higher in the rear suspension is its distance from other important noise sources; the chassis accelerometer in the front suspension is close to both the motor housing and front A-pillar and wing mirror, both of which may be significant noise sources.

3.2. Effect of road surface

The results presented so far were averaged over the entire data set that was collected while driving on local roads. Although the data was collected under consistent driving conditions (at approximately 30 mph on similar roads), the roughness of the road surface would be expected to vary between segments of data. The suspension's response to different road surfaces (i.e., different input amplitudes) is of interest since, if the suspension's dynamics are significantly nonlinear, it could vary on smooth and rough roads. Nonlinear processes might appear to be approximately linear under low amplitude excitations, whereas for larger inputs, the nonlinearity can be exhibited more strongly. Coherence can give a measure of nonlinearity if no unmeasured noise sources are present in the measurements; a lower coherence on rougher road segments might therefore be further evidence of nonlinear suspension behaviour. This section presents an analysis of the measurements in the car when divided into small and large amplitude frames of data. The presence of unmeasured noise sources in the car measurements, whose influence cannot be easily quantified, means that only tentative conclusions can be drawn from these results.

First, a method for defining small and large amplitude road inputs is required: the data was split into overlapping frames of 2^{15} samples (1.6 s), and the rms amplitude of the vertical displacement at the front left wheel hub was

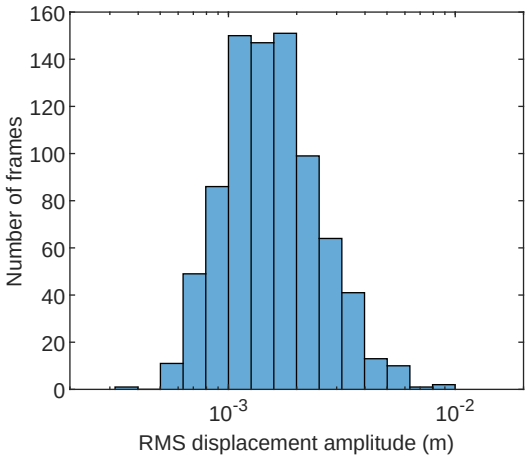

Figure 6: Histogram of the rms displacement in the vertical axis at the front left wheel hub, calculated for each frame of data.

calculated for each frame. Figure 6 shows the rms amplitudes of each frame plotted as a histogram. When the bin widths are spaced logarithmically, the distribution is approximately symmetrical with a mean of 1.75 mm. The frames were then divided into 'smooth' and 'rough' road categories; the lowest amplitude third were classed as 'smooth' roads, and the largest amplitude third were classed as 'rough' roads. This split was chosen to ensure that the two categories had enough frames for coherence estimates to converge.

Figure 7a shows the multiple coherence between the 12 wheel hub channels and the microphone positioned at the front passenger's left ear. The coherence is shown for 'smooth' roads (dashed, blue) and 'rough' roads (dot-dashed, red), as well as when all frames are used in the calculation (solid, grey). In some frequency ranges (e.g. 60-80 Hz, > 200 Hz), the three lines are very close and the coherence does not appear to be affected by the road surface. However in other regions (e.g. 30-60 Hz, 80-200 Hz), there is a significant difference. The coherence is highest for the 'smooth' road category in these regions, whereas the 'rough' road category generally has the lowest coherence. This suggests that, in the frequency ranges where the blue line is highest, some nonlinear road noise may be transmitted into the cabin. However, this is not conclusive since the role of other noise sources can not be easily quantified in the measurements. Figure 7b shows the coherence limits corresponding to Fig. 7a. The difference in the theoretical maximum cancellation possible on 'smooth' and 'rough' roads is approximately 2-3 dB between 30-60 Hz and 2 dB between 80-200 Hz.

If nonlinear suspension dynamics are the cause of the trend seen in Fig. 7, a similar pattern should be seen in the coherences to the chassis and damper piston rod measurement locations in the suspension. These measurements should also be less affected by noise from other sources than the microphone measurements, so can provide useful insight. Figure 8a shows the multiple coherence between all the wheel hub signals and the vertical (z) axis of the front left damper piston rod; again, the coherence is shown for 'smooth' roads (dashed, blue), 'rough' roads (dot-dashed, red) and all frames (solid, grey). At nearly every frequency, the coherence is highest for the 'smooth' road category and lowest for the 'rough' road category. The difference between the two classes is largest between 50-160 Hz. Interestingly, the coherence calculated with all of the frames (solid, grey) is much closer to the coherence for the 'rough' road category, apart from between 70-110 Hz; this might be partly explained by the fact that the coherence is calculated from the PSDs of the signals, whose magnitude is quadratically related to the time domain amplitudes of the signals. A change in amplitude of one of the signals would therefore lead to a disproportionate change in coherence. Figure 8b shows the multiple coherence to the chassis measurement location. A similar trend can be seen, with the coherence highest for the 'smooth' road category over the entire frequency range. Once again, the coherence calculated with all of the frames is similar to the 'rough' road category.

The trends observed on 'smooth' and 'rough' roads point towards nonlinear suspension behaviour being responsible for the low measured coherence. However, the influence of other noise sources can not be discounted in these analyses and so the results should be treated with a degree of caution. Although most of the data was collected while

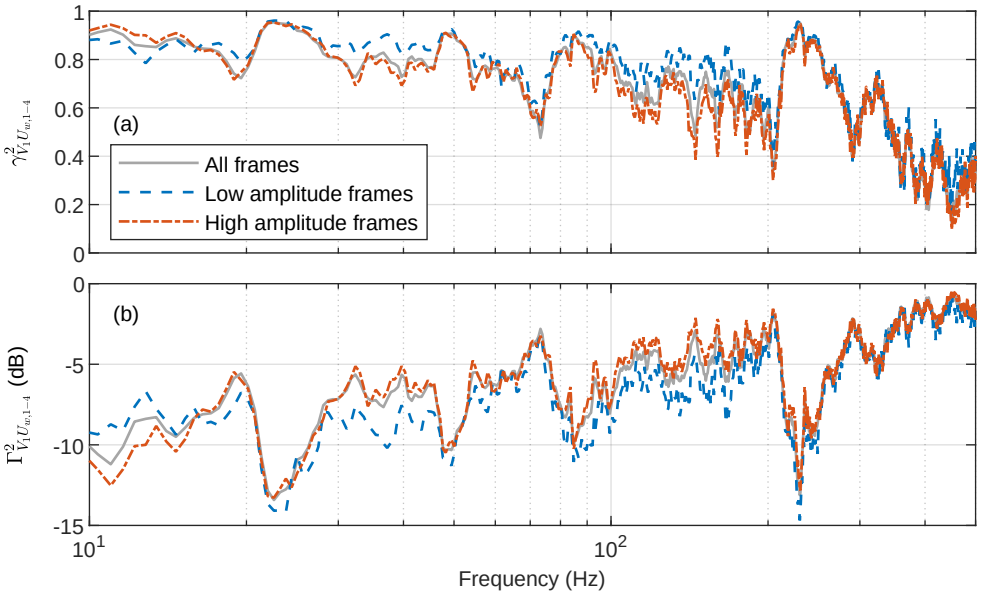

Figure 7: (a) Multiple coherence and (b) coherence limit between the wheel hubs and left microphone, when calculated on 'smooth' roads (blue) and 'rough' roads (red).

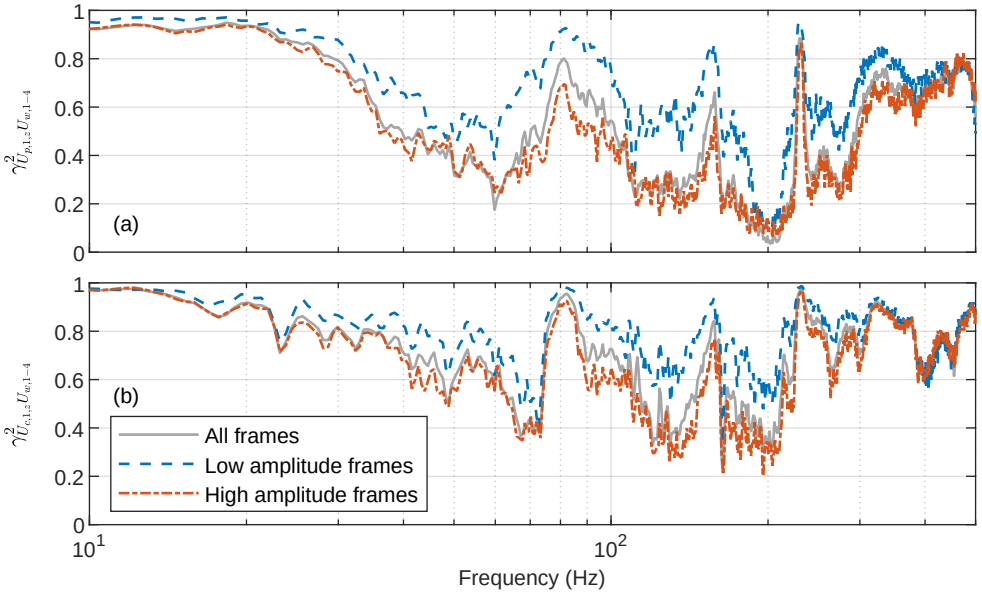

Figure 8: Multiple coherence between the wheel hubs and (a) front left damper piston rod (vertical axis) and (b) front left damper chassis (vertical axis), when calculated on 'smooth' roads (blue) and 'rough' roads (red).

driving at close to 30 mph, some segments of data may have been recorded at slightly slower speeds (20-25 mph). The frames were classified as being 'smooth' or 'rough' according to the rms displacement in the vertical axis at the front left wheel. This is a potential source of error in the analysis, particularly if there is a correlation between slower vehicle speeds causing smaller wheel hub displacement amplitudes. This is because when the vehicle is travelling slower, other unmeasured noise sources (e.g., wind noise) might be less significant, which in turn would affect the coherences calculated with the experimental data. Nonetheless, the wheel hub displacement is mostly dependent on the road roughness profile and it is not clear that it would be affected by small variations in vehicle speed. The assumption made in the definition of the 'smooth' and 'rough' categories therefore seems reasonable. When viewed alongside the coherence plots calculated with different combinations of input signals, the measurements on the suspension do point towards nonlinear suspension dynamics being significant and limiting the performance of a linear controller.

4. Suspension component tests

In the car a large number of noise sources are present, and it was not possible to measure them all and therefore quantify their significance. This made it impossible to firmly attribute the low measured coherence to nonlinearity in the suspension systems since the other, unmeasured noise sources may have been responsible. This section describes laboratory experiments conducted on components from the Nissan Leaf's suspension systems to quantify the extent of their nonlinear characteristics. When testing under laboratory conditions it is easier to measure the undesired noise sources and mitigate their effect.

The experiments were conducted with an Instron 8872 fatigue testing frame that was driven by an Instron 8800MT controller, shown in Fig. 9. The servohydraulic actuator is controlled to follow a prescribed displacement input and can apply both harmonic and broadband inputs. The system has its own DAQ system that enables measurements from a load cell and displacement sensor. However, the noise floor of the displacement sensor was found to be too high to give good quality measurements above 100 Hz. Consequently, additional accelerometers were added to the system to provide measurements of displacement. The accelerometers and force signal were connected to the same DAQ system as was used in the car, described in Section 2. Data was logged at 20 kHz to be consistent with the car measurements, although sensor noise from the Instron meant that the laboratory measurements were only reliable up to 300 Hz.

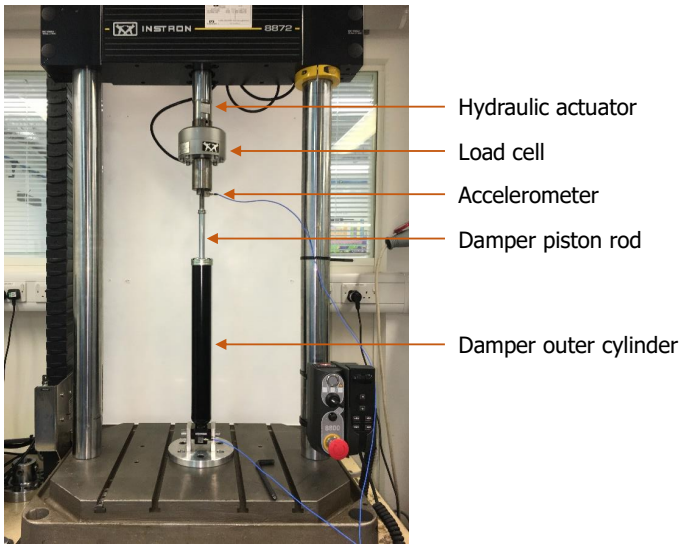

Figure 9: Rear damper installed in the Instron test system.

To assess the importance of the nonlinear suspension characteristics, a measure of nonlinearity is required. The coherence between the input displacement and output force was used for this purpose. In a single-input single-output system, the coherence predicts the fraction of the output that is linearly correlated with the input [29]. A decrease in coherence could be caused either by nonlinear system behaviour or uncorrelated, unmeasured noise sources in the

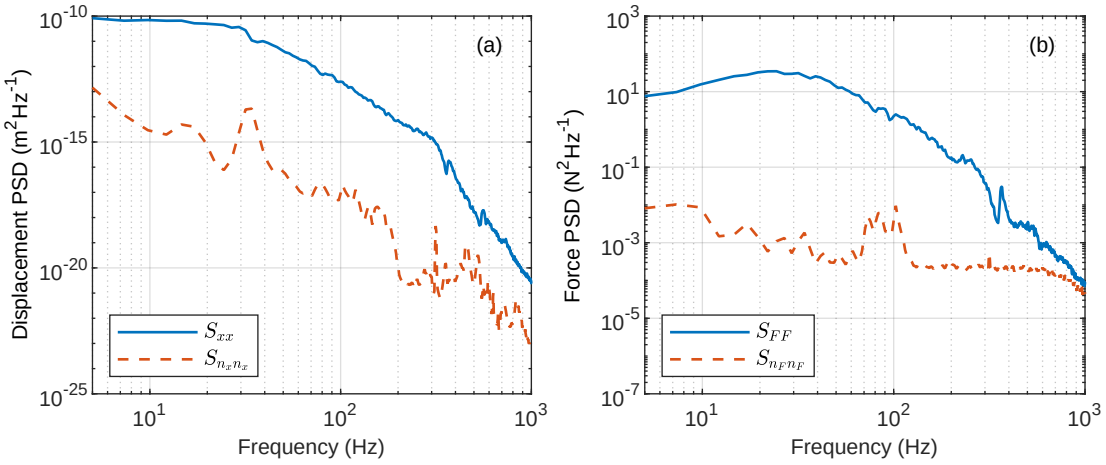

Figure 10: (a) Displacement and (b) force PSDs (blue) with noise floor measurements (red).

input or output. By testing the suspension components in a laboratory, the influence of uncorrelated noise sources can be controlled and quantified. In the experiments with the Instron the only uncorrelated source is electrical noise from the sensors and DAQ system. A signal-to-noise analysis was conducted to estimate how much of the decrease in coherence is caused by electrical noise; the remaining decrease must then be due to nonlinearity.

To quantify the role of electrical noise, the force and acceleration channels were recorded with no input to the system. PSDs were calculated for the sensor noise in each channel, which are denoted by $S_{n_F n_F}$ and $S_{n_x n_x}$. Figure 10 shows PSDs of (a) displacement and (b) force measured during a test, along with the corresponding noise measurements. These can then be combined to obtain an estimate of coherence as if the system were linear, so any decrease is therefore caused by sensor noise. The coherence between the force, F, and displacement, x, is calculated as

$$\gamma^2_{xF} = \frac{|S_{xF}|^2}{S_{xx} S_{FF}}. \tag{4}$$

The decrease in coherence due to sensor noise is estimated from the measured PSDs as

$$\bar{\gamma}^2_{xF} = \frac{(S_{xx} - S_{n_x n_x})(S_{FF} - S_{n_F n_F})}{S_{xx} S_{FF}}. \tag{5}$$

Data was once again logged at 20 kHz and each measurement lasted 30 s. The PSDs were calculated in the same way as described in Section 3.1 but with a frame length of 0.41 s (2^{13} samples). This means that 145 frames contribute to the averaged PSDs for each 30 s data set.

The components that were tested were the front and rear dampers and the front top mount bushing. The front damper and top mount were also tested when coupled together as they are in the car; the damper piston rod (the upper part of the damper) bolts directly to the inner part of the bushing as in Fig. 2c. This configuration is referred to as the front strut. Both the front and rear suspensions contain two further bushings on each side of the car. These were not tested due to practicality issues, however, the results of the top mount tests are expected to be representative of the other bushings. All the bushings were tested statically, and their stiffnesses only become nonlinear at large displacements [30]. The dynamic tests on the top mount bushing were conducted at amplitudes that were similar to those measured in the car, at which its geometric nonlinearity is not activated. Any nonlinear behaviour observed in the dynamic test on the top mount bushing is therefore caused by its material properties, which are the same for the other bushings. Results for the structural components in the suspension (such as the spring and wishbone) are also not presented here as these are expected to be linear.

If the tested components turn out to be nonlinear then their response will vary depending on the input that is applied. It was therefore necessary to apply inputs with similar amplitudes and frequency content as the displacements observed in the car. Displacement signals were derived from the accelerometer measurements on the car. The

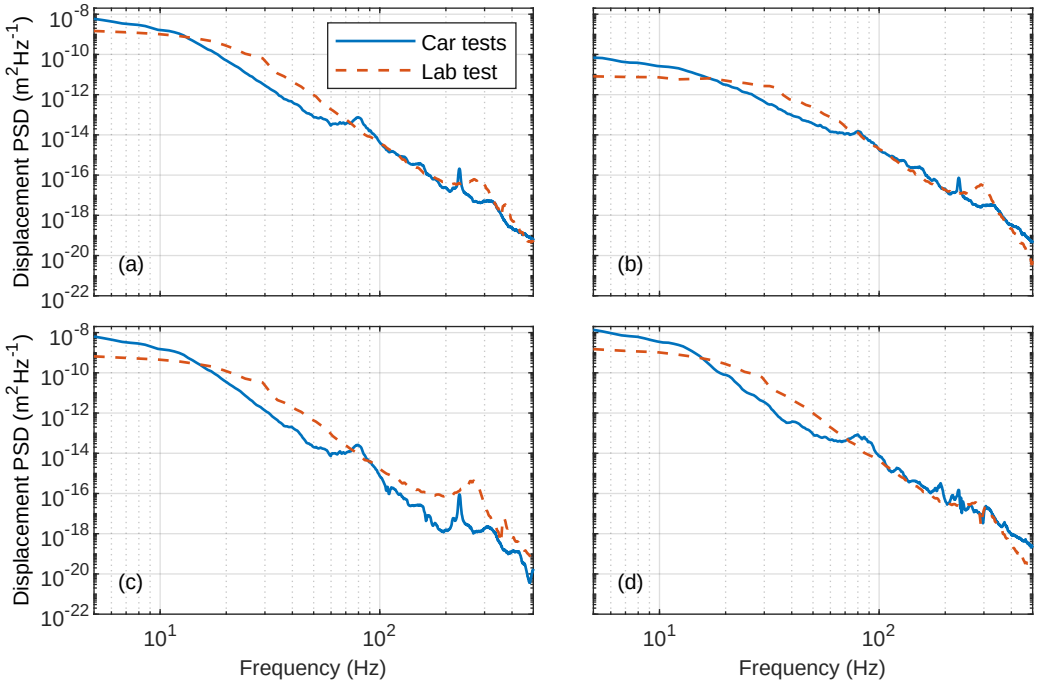

Figure 11: Comparison between displacements measured in the car and input in the lab tests for (a) the front damper (b) the front top mount (c) the front strut and (d) the rear damper.

displacement inputs to the dampers were estimated from the relative accelerations in the vertical axis between the wheel hub (u_w) and damper piston rod (u_p) accelerometers in the front and rear left suspensions. The top mount input was derived from the relative acceleration between $u_{p,1,z}$ and $u_{c,1,z}$, and the strut input was estimated from the relative acceleration between $u_{w,1,z}$ and $u_{c,1,z}$. The relative accelerations were then high-pass filtered, to remove drift, and integrated twice to obtain estimates of displacement. This method has some disadvantages, in that the very low frequency component ($<$ 2 Hz) of the signal is lost. Furthermore, as the wheel hubs rotate around the bushings the accelerometers u_w could detect either a time varying component of gravity or a centripetal acceleration. However, for the purpose of this study an estimate of displacement is sufficient since the Instron was not capable of reproducing the exact specified inputs. Figure 11 shows a comparison between the averaged displacements measured across each component in the car (solid, blue) and the most similar tests conducted with the Instron (dashed, red). In general, the displacements applied in the Instron are smaller at low frequencies, but similar above 70 Hz. The Instron can not reproduce some of the details of the measured road responses, such as the peaks resulting from tyre modes at approximately 80 Hz and 230 Hz. However, the shape and amplitude of the measured spectra are broadly reproduced, which should provide insight into the role of nonlinearity in the suspension's dynamics. In the lab test PSDs, the first mode of the test system can be seen around 280 Hz. Above this frequency, the dynamics of the test frame become significant and the signal-to-noise ratio deteriorates so the results are less reliable.

The force measurements corresponding to the inputs shown in Fig. 11 were used to estimate the coherence. The coherence plots are shown in Fig. 12 along with the signal-to-noise analyses. In each test, the maximum expected coherence (given the estimated noise floor), $\bar{\gamma}^2_{xF}$, is very close to 1 up to approximately 300 Hz. This indicates that uncorrelated electrical noise was insignificant in this frequency range. In contrast, the coherence between force and displacement, γ^2_{xF}, is significantly less than the noise floor coherence, $\bar{\gamma}^2_{xF}$, which must be caused by nonlinearity. For both the front and rear dampers, coherence is particularly low between 70 and 200 Hz. This indicates that nonlinearity is very significant in the transmission of low audio frequency vibrations through these components. The coherence across the top mount bushing (Fig. 12b) is much higher than either of the dampers. At 300 Hz, $\bar{\gamma}^2_{xF}$ is 0.98 and γ^2_{xF} is 0.92. This implies that the top mount bushing is only weakly nonlinear for the input levels that are seen in the

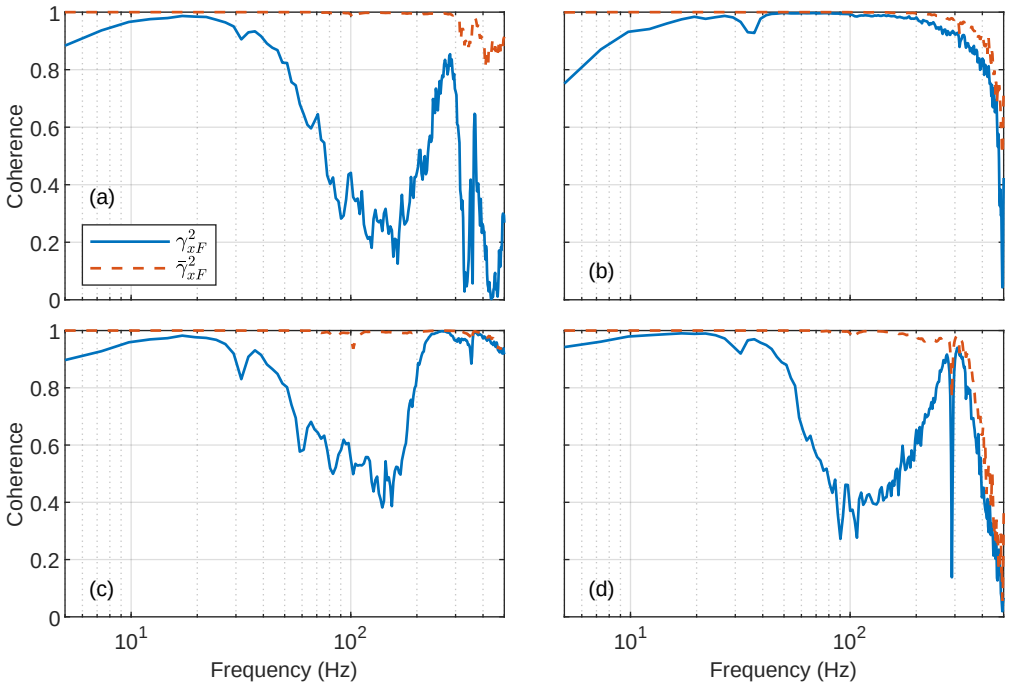

Figure 12: Coherence between x and F measured in the lab tests for (a) the front damper (b) the front top mount (c) the front strut and (d) the rear damper.

car. When the top mount bushing was coupled to the front damper, the coherence showed features of both individual components (Fig. 12c). At low frequencies, the damper appears 'soft' and so dominates the strut's response. This explains the decrease in coherence starting from approximately 40 Hz. At high frequencies, the dynamic stiffness of the damper increases and the top mount bushing dominates the strut's response, which is why the coherence improves to close to one above 150 Hz. In the front strut configuration, the damper and top mount bushing are bolted together; the bolted joint introduces an additional source of nonlinearity which might have also contributed to the low coherence.

For the excitation levels measured in the car, the dampers in the front and rear suspensions are significant sources of nonlinearity in the road noise transmission path and therefore appear to limit the performance of a RNC system. However, the significance of vibration transmission through the vertical strut (relative to the other transmission paths) is not yet known; if the vertical struts transmit much less road noise into the cabin than the other more linear paths, then the uncorrelated (with the wheel hubs) road noise in the cabin could be insignificant. Nevertheless when all the experimental results are viewed together, they strongly suggest that nonlinear suspension behaviour limits the cancellation that can be achieved with a linear feedforward RNC system. The frequency range in which low coherence was observed during the laboratory tests on the dampers (40-300 Hz, Fig. 12a,c) coincides with the regions of low coherence seen in the suspension measurements (20-80 Hz and 100-230 Hz, Figs. 4 and 5) and acoustic measurements (50-80 Hz and 100-230 Hz, Fig. 3) on the car. The top mount bushing was found to be very weakly nonlinear and is thought to be representative of the other bushings in the road noise transmission path. When the front damper and top mount bushing are coupled together, vibration transmission across these components is still strongly nonlinear at low audio frequencies. This suggests that the trends in coherence observed in the car measurements in Section 3 are caused by nonlinear suspension dynamics that are mainly driven by the hydraulic dampers.

5. Conclusions

Two sets of experiments have been presented that aim to explore whether structure-borne road noise transmission is nonlinear and therefore limits the cancellation possible with a linear control system. In the first set of experiments,

measurements were obtained of vibration on the suspensions and sound in the cabin of an electric car. Two sets of multiple coherence calculations were then presented in which: the reference sensors used as inputs to the calculation were varied; and the data was split into 'smooth' and 'rough' road surface categories, with coherence calculated for these subsets. Together, these results suggest that vibration transmission through the suspensions is nonlinear. However, this can not be stated with certainty since the measurements contain noise from other, unmeasured sources (e.g, wind and power train noise).

To overcome this limitation, a second set of experiments was conducted in a laboratory. Components from the car's suspensions were tested with inputs that were comparable with the excitation levels measured in the car when driven at approximately 30 mph. In these experiments, the influence of unmeasured noise sources (i.e., sensor noise) can be controlled and quantified, meaning the significance of the components' nonlinear characteristics can be accurately quantified. The laboratory tests show clearly that, for the excitation levels observed in the car during driving, the hydraulic dampers are the most strongly nonlinear components in the suspensions. In comparison, the top mount bushing was found to be only very weakly nonlinear. The evidence from the two sets of experiments is that road noise transmission is significantly nonlinear in the low audio frequency range (50-500 Hz) in which it is most significant, and that the nonlinearity arises primarily from the hydraulic dampers. This nonlinearity appears to significantly limit the cancellation that can be achieved with a linear system using a limited number of reference sensors.

Acknowledgements

The authors would like to thank Bose Corporation for funding this research and Professor Robin Langley for the many helpful discussions.

References

[1] T. Priede, Origins of automotive vehicle noise, Journal of Sound and Vibration 15 (1) (1971) 61–73. doi:10.1016/0022-460X(71)90360-9.
[2] F. Fahy, J. Walker, Advanced applications in acoustics, noise, and vibration, Spon Press, 2004.
[3] D. Crolla, Automotive Engineering: Powertrain, Chassis System and Vehicle Body, Elsevier, 2009.
[4] T. Sutton, The Active Control of Random Noise in Automotive Interiors, Ph.D. thesis, University of Southampton (1992).
[5] S. J. Elliott, P. A. Nelson, Active Noise Control, IEEE Signal Processing Magazine 12–35.
[6] S. J. Elliott, A Review of Active Noise and Vibration Control in Road Vehicles, Tech. rep.
[7] U. Stöbener, L. Gaul, Active vibration control of a car body based on experimentally evaluated modal parameters, Mechanical Systems and Signal Processing 15 (1) (2001) 173 – 188. doi:https://doi.org/10.1006/mssp.2000.1325.
[8] S. Hurlebaus, U. Stöbener, L. Gaul, Vibration reduction of curved panels by active modal control, Computers & Structures 86 (3) (2008) 251 – 257, smart Structures. doi:https://doi.org/10.1016/j.compstruc.2007.01.036.
[9] T. Sutton, S. J. Elliot, M. McDonald, T. Saunders, Active control of road noise inside vehicles, Journal of Noise Control Engineering 42 (4) (1994).
[10] W. Jung, S. J. Elliott, J. Cheer, Combining the Remote Microphone Technique with Head-tracking for Local Active Sound Control, Journal of the Acoustical Society of America 142 (2017) 5403.
[11] W. Jung, S. J. Elliott, J. Cheer, Local active control of road noise inside a vehicle, Mechanical Systems and Signal Processing 121 (2019) 144–157. doi:10.1016/j.ymssp.2018.11.003.
[12] T. Inoue, A. Takahashi, H. Sano, M. Onishi, Y. Nakamura, NV Countermeasure Technology for a Cylinder-On-Demand Engine- Development of Active Booming Noise Control System Applying Adaptive Notch Filter, SAE Technical Papers (2004).
[13] R. Schirmacher, R. Kunkel, M. Burghardt, Active noise control for the 4.0 TFSI with cylinder on demand technology in Audi's S-series, in: SAE Technical Papers, 2012. doi:10.4271/2012-01-1533.
[14] S. Hasegawa, T. Tabata, A. Kinoshita, H. Hyodo, The Development of an Active Noise Control System for Automobiles, in: SAE Technical Paper No. 922086, 1992. doi:10.4271/922086.
[15] W. B. Ferren, R. J. Bernhard, Active Control of Simulated Road Noise, in: SAE Technical Paper No. 911046, 1991. doi:10.4271/911046.
[16] S. H. Oh, H. S. Kim, Y. Park, Active control of road booming noise in automotive interiors, The Journal of the Acoustical Society of America 111 (101) (2002). doi:10.1121/1.1420390.
[17] J. Duan, M. Li, T. C. Lim, M. R. Lee, M. T. Cheng, W. Vanhaaften, T. Abe, Combined feedforward-feedback active control of road noise inside a vehicle cabin, Journal of Vibration and Acoustics, Transactions of the ASME 136 (4) (2014). doi:10.1115/1.4027713.
[18] N. Zafeiropoulos, M. Christoph, J. Zollner, V. Kandade Rajan, Active control of structure-borne road noise: A control strategy based on the most significant inputs of the vehicle, in: INTER-NOISE and NOISE-CON Congress and Conference Proceedings, 2016.
[19] P. Sas, W. Dehandschutter, Active structural and acoustic control of structure-borne road noise in a passenger car, Noise and Vibration Worldwide (1999).
[20] N. Zafeiropoulos, A. Moorhouse, A. Mackay, M. Ballatore, Active control of road noise: the relation between the reference sensor locations and the effect on the controller's performance, in: ICSV22: The 22nd International Congress of Sound and Vibration, 2015.
[21] J. Cheer, S. J. Elliott, Multichannel control systems for the attenuation of interior road noise in vehicles, Mechanical Systems and Signal Processing 60 (2015) 753–769. doi:10.1016/j.ymssp.2015.01.008.

[22] S. Duym, K. Reybrouck, Physical characterisation of nonlinear shock absorber dynamics, European Journal of Mechanical and Environmental Engineering 43 (4) (1998) 181–188.
[23] V. Y. B. Yung, D. J. Cole, Modelling high frequency force behaviour of hydraulic automotive dampers, Vehicle System Dynamics 44 (1) (2006) 1–31. doi:10.1080/00423110500171125.
[24] M. Benaziz, S. Nacivet, F. Thouverez, A shock absorber model for structure-borne noise analyses, Journal of Sound and Vibration 349 (2015) 177–194. doi:10.1016/j.jsv.2015.03.034.
[25] M. J. García Tárrago, L. Kari, J. Vinolas, N. Gil-Negrete, Frequency and amplitude dependence of the axial and radial stiffness of carbon-black filled rubber bushings, Polymer Testing 26 (5) (2007) 629–638. doi:10.1016/j.polymertesting.2007.03.011.
[26] W. P. Fletcher, A. N. Gent, Nonlinearity in the Dynamic Properties of Vulcanized Rubber Compounds, Rubber Chemistry and Technology 27 (1) (1954) 209–222. doi:10.5254/1.3543472.
[27] A. R. Payne, R. E. Whittaker, Low Strain Dynamic Properties of Filled Rubbers, Rubber Chemistry and Technology 44 (2) (1971) 440–478. doi:10.5254/1.3547375.
[28] J. C. Dixon, The shock absorber handbook, Wiley, 2007.
[29] J. S. Bendat, A. G. Piersol, Random data: analysis and measurement procedures, Wiley, 2010.
[30] M. de Brett, Implications of nonlinear suspension behaviour for feedforward control of road noise in cars, Ph.D. thesis, University of Cambridge (2020).